International Journal of Applied Engineering Research ISSN 0973-4562 Volume 13, Number 10 (2018) pp. 7477-7487

Experimental Investigation and Effective Medium Approximation of Thermal Conductivity of Water Based Exfoliated Graphene Nanofluids

A. Arifutzzaman[1*], A. F. Ismail[2], I. I. Yaacob[1], A. A. Khan[1] and M. Z. Alam[3]

[1]Department of Manufacturing and Materials Engineering, International Islamic University Malaysia, Kuala Lumpur, Malaysia.
[2]Department of Mechanical Engineering, International Islamic University Malaysia, Kuala Lumpur, Malaysia.
[3]Department of Biotechnology Engineering, International Islamic University Malaysia, Kuala Lumpur, Malaysia.

**corresponding author*

Abstract

In this work Graphene (Gr) flake was exfoliated using the solvents N-Methyl-2-Pyrrolidone (NMP) and processed by systematic centrifugation. Raman spectroscopy and Field Emission Scanning Electron Microscopy (FESEM) analysis were conducted for the characterization of as fabricated Gr flakes. Exfoliated Gr was re-dispersed into the deionized water (DW) with the aid of vacuum filtration process. Then five different nanofluid samples were prepared by dispersing Gr in DW (Gr/DW). In these samples volume fractions of Gr were varied from 0.10 to 0.30 % in DW. Systematic thermal conductivity (TC) measurements were conducted separately on the prepared Gr dispersed nanofluid samples. Prediction of TC enhancements for Gr/DW nanofluids were explained by analytical explanation with the modification of effective medium approach (EMA). In the approximation low filling of Gr flake and its random orientation were taken into consideration with the effect of ultrathin Gr fake's basal plane TC. The model predictions agreed very well with the measured TCs of as produced exfoliated Gr/DW nanofluids. It was shown that, using exfoliated Gr flakes of extremely wide basal plane with negligible thickness and non-flat or crumpled ratio was an efficient factor to obtain the considerably better agreement with the TC enhancements of Gr/DW nanofluids.

Keywords: graphene, nanofluids, thermal conductivity, effective medium approximation, prediction of thermal conductivity

INTRODUCTION

Thermal properties of different nanofluids have been studied comprehensively [1]. Thermal conductivity (TC) has been drawing the extreme consideration among all other thermal properties of nanofluids. It is considered as the most crucial factor for the heat transfer in nanofluids [2]. Effective TC behaviors are significantly desirable during the uses of nanofluids in different practical thermal devices such as, the new kind of heat exchangers, cooling loops and energy conversion systems along with the structural and microelectronic packaging materials.

Addition of high thermal conductive particles in the liquids enhances the TC of new fluids Maxwell (1881) [3]. It leads to generate the idea of addition of Gr nanosheets in the conventional heat transfer fluid such as water for the enhancement of TC. One atom thick Gr nano-sheet is an ultra-thin carbon film [4]. Often, it is defined as the structures of three or few layers of Gr sheets [5]. It is the most promising nanomaterial because of the exponentially high thermo-electrical conductivity, high mobility of charge carriers and high mechanical strength along with the enormously large surface area [6]. Two-dimensional form of single atomic layer Gr have exhibited high crystal quality and to have ballistic thermal conductance [7]. Chemical processing such as liquid-phase exfoliation (LPE) of graphite has shown the most anticipation to produce Gr suspension in organic solvents [8, 9, 10, 11, 12]. Microcrystalline graphite particles can exfoliate into separate Gr sheets in the solvent with the aid of sonication by generating the shear forces and cavitation in solvent [13, 14]. To some extant heat transfer mechanism in Gr nanofluids is similar to carbon nanotube (CNT) containing nanofluids [6]. However, transferring heat in nanofluids, Gr could outperform because of its excessively high TC than the CNTs [15, 16, 17]. Shahil and Balandin, (2012) [18] experimentally confirmed that Gr is better filler than CNT in terms of TC enhancements. One of the vital reasons is that, Gr possesses far smaller thermal boundary resistance in fluids than the CNT [19,18]. Comparison of modern nanotechnology and orthodox thermal science shown that, TC of Gr nanosheets suspended nanofluids provide a significant potential and regarded as an attractive candidate for next-generation materials in heat transfer application [6,20].

It is found in literature that, theoretical predictions of TCs by conventional effective medium theories are awfully under predicted from the experimentally measured TCs of the carbon based material dispersion [21, 22]. In this regards anomalous behavior of TC enhancement for these dispersions are theoretically very fascinating. Although heat transport behavior nearly similar for Gr and CNT [6]. Some theoretical analyses have presented in literature to explain the heat transport behavior of CNT dispersed nanofluids. However, implementations of theoretical approach have not widely used to predict the TC enhancement behavior of Gr flake dispersed nanofluids. Therefore, the objective of this work is to experimentally investigate the TC and modification of effective medium theories for the analysis of TC behaviour of the exfoliated Gr suspended DW nanofluids. The influencing factor volume fraction of Gr flakes was also explained.

Theory of Effective Medium Approximation for Thermal Conductivity of Nanofluids

At 1881, Maxwell, (1881) [3] investigated the conduction of liquid suspensions analytically by considering a very dilute suspension containing spherical particles and ignoring the interactions among particles. It was developed for the continuum medium of dispersed micro- or mili-sized solid particles. In this model, it was not considered the effects of particle size, interfacial nanolayer at the particle-liquid interface and motion of particles. The Maxwell model is used as the representative of traditional models. Well-known Maxwell theory for the effective TC, K_{eff} of the particle dispersed liquid suspensions is expressed as Equation 1 [1, 3, 23].

$$K_{eff} = \frac{(K_p + 2K_f) + 2\varphi(K_p - K_f)}{(K_p + 2K_f) - \varphi(K_p - K_f)} \times K_f \quad \ldots\ldots\ldots\ldots\ldots\ldots (1)$$

where, K_{eff} is the effective TC of the suspension; K_p is the TC of the solid particles, K_f is the TC of the base fluids; φ is the volumetric fraction of the solid particles as filler.

It is found that Nan, (1993) [24] used multiple shattering approaches for effective medium theory. Latter, it was introduced an effective medium theory by considering a composite medium whose TC varies from point to point. The variation of TC consist with two parts, between them one is from constant part of a homogeneous medium and other part is generated from the arbitrary fluctuating part related with the interaction between particles which was neglected in the approximation for the simplicity of calculation. Apparently, this approximation was only effective for the dispersion where solid particles are dispersed in the matrix (based fluid) [25, 26].

Nan, et al., (1997) [26] considered two-phase composite containing ellipsoidal fillers with considering interfacial thermal resistance existing between the matrix and filler, in which the materials axes are denoted by X_i and the local, oriented axes by X_i' with X_3' corresponding with the symmetric axis of the filler particles considered. Figure 1 shows the schematic illustration of the dimensions of spherical (oblate and prolate spheroid) filler geometry.

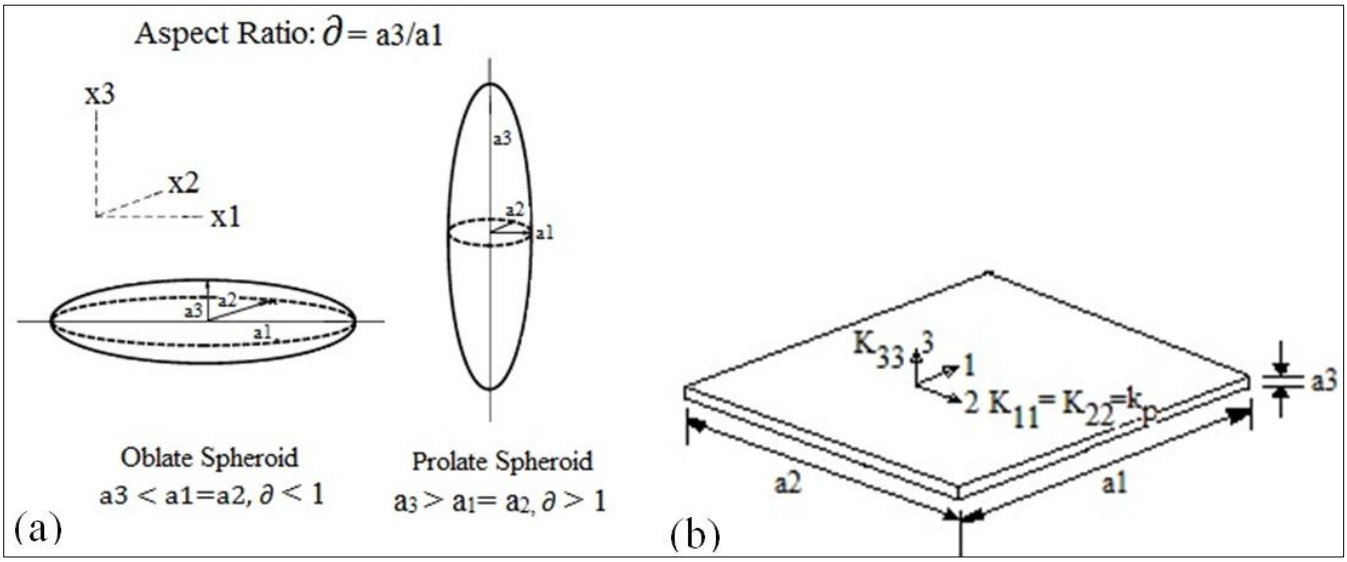

Figure 1: Schematic illustration (a) dimensions of oblate and prolate spheroid, (b) composite unit cell of a Graphene flat plate indicating that $a_1=a_2 >> a_3$. The equivalent TC along the basal plane of the plate is K_{11} (= K_{22}) = K_p and TC normal to the basal plane is K_{33}.

Nan et al., (2003) [25] and Nan, et al., (1997) [26], formulate the Effective Medium Approximation (EMA) for arbitrary ellipsoidal particulate composites. Maxwell Gantt Effective Medium Approximation (MG-EMA) was rediscovered by considering interfacial thermal resistance [22, 27] for the several ellipsoidal particle geometry, topologies and orientations in the matrix. The solid particle and matrix interface is assumed to be effective for the transport of energy across it. If is taken the matrix phase as the homogeneous reference medium, so K_f presence as the TC of the matrix (base fluid). Then, the recovered MG type EMA of the theory for the effective TC, K_{eff} of the system with equalized ellipsoidal particles as,

$$K_{eff} = K_f \frac{2 + \varphi_p[\beta_{11}(1 - L_{11})(1 + \langle Cos^2\theta\rangle) + \beta_{33}(1 - L_{33})(1 - \langle Cos^2\theta\rangle)]}{2 - \varphi_p[\beta_{11}L_{11}(1 + \langle Cos^2\theta\rangle) + \beta_{33}L_{33}(1 - \langle Cos^2\theta\rangle)]}$$

…… (2)

L_{ii} is the well-known geometrical factors based on the principal axes of non-spherical (spheroid) particles dependent on the shape of the particle assumed by Nan, (1993) [24] and

Nan, (1994) [28]. L_{ii} is expressed as the function of aspect ratio of non-spherical filler by Nan, et al., (1997) [26],

$$L_{11} = L_{22} = \begin{cases} \frac{\partial^2}{2(\partial^2-1)} - \frac{\partial}{2(\partial^2-1)^{3/2}}\cosh^{-1}\partial, & for \quad \partial > 1, \\ \frac{\partial^2}{2(\partial^2-1)} + \frac{\partial}{2(1-\partial^2)^{3/2}}\cos^{-1}\partial, & for \quad \partial < 1, \end{cases}$$

And $L_{33} = 1 - 2L_{11}$

…… (3)

where, $\partial = a_3/a_1$ is the aspect ratio of the ellipsoid. Aspect ratio, $\partial < 1$ is for an oblate spheroid where $a_3 < a_1 = a_2$, on the other hand, $\partial > 1$ is for a prolate spheroid where $a_3 > a_1 = a_2$ [18, 26].

β_{ii} is the function of TC β_{ii} could be defined as [25, 26, 29],

$$\beta_{ii} = \frac{K_p - K_f}{K_f + L_{ii}(K_p - K_f)]}$$

……..…….. (4)

The average $\langle Cos^2\theta \rangle$ is given by (Nan, et al., 1997 [26], Nan, et al., 2000 [30]),

$$\langle Cos^2\theta \rangle = \frac{\int \rho(\theta)\ \cos^2\theta\ \sin\ \theta\, d\theta}{\int \rho(\theta)\ \sin\ \theta\, d\theta}$$

..……..…… (5)

where, θ is the angle between the materials axis X_3 and the local particle symmetric axis X_3', $\rho(\theta)$ is a distribution function describing ellipsoidal particle orientation and φ is the volume fraction of particles. Equation 2 can be treated as the common EMA formulations that comprehend the effects of particle size, shape, orientation distribution, volume fraction, interfacial thermal resistance as well as K_p and K_f on K_{eff} of the suspension. From equation 2 shortened expressions for K_{eff} can be straightforwardly given for several types of filler geometry and topologies.

Modification of Effective Medium Theory

We assumed that the fillers are randomly oriented in the based fluid. It is also supported in by Shahil and Balandin, (2012) [18]. Then the average geometrical factor in Equation 5, $\langle Cos^2\theta \rangle$ =1/3 [26]. In this situation, the effective TC, K_{eff} of the dispersion is obtained from equation 2 as,

$$K_{eff} = K_f \frac{3 + \varphi_p[2\beta_{11}(1-L_{11}) + \beta_{33}(1-L_{33})]}{3 - \varphi_p[2\beta_{11}L_{11} + \beta_{33}L_{33}]}$$

……..……..… (6)

Equation 6 is a desired general MG-EMA formulation for the TC enhancement of the arbitrary isotropic particulate dispersion, which includes the effects of the diameter, aspect ratio and volume fraction of the filler and also the effect of interface thermal resistance, and TC ratio of K_p/K_f on the effective TC of the dispersion.

Both Gr flakes and CNTs can be considered as spheroids with principle dimensions a1=a2 and a3. An ideal Gr flake can be treated as an oblate spheroid with ∂ = a3/a1→0 [18], (as because a1=a2 >> a3) which means, the Gr flake possesses ultra large basal plane dimensions (a1=a2) comparing to negligible thickness normal to the basal plane direction (a3). While CNT is treated as a prolate spheroid with $\partial \to \infty$ (with a1=a2<<a3). This difference in ∂ was theoretically predicted to make Gr much better filler than CNTs [18, 31]. Considering this negligible aspect ratio, Gr flake can be treated as a flat plat (as in Figure 1b). For flat plate, the geometrical factors is given $L_{11} = 0$ so $L_{33} = 1$ (from Equation 3) given by Nan, et al., (1997) [26].

Then from equation 4, β_{11} and β_{33} can be written as,

$$\beta_{11} = \frac{K_p}{K_f} - 1$$

……..……..… (7)

$$\beta_{33} = 1 - \frac{K_p}{K_f}$$

……..……..… (8)

As for Gr flake $K_p >> K_f$. In the dilute limit as in the carbon based material dispersed nanocomposite is reported in the literature, (e.g., $\varphi < 1$) [21, 22, 24, 25, 29, 30, 32].

Now, implementing all these conditions in equation 6, TC enhancement of Gr flake suspended nanofluids is modified as,

$$\frac{K_{eff}}{K_f} = 1 + \frac{2}{3}\varphi\ \frac{K_p}{K_f}$$

…… (9)

Actually, only one isotropic TC, K_p was observed for in the Gr flakes. This quite simple relation in Equation 9 clearly demonstrates the large TC enhancement induced by the high TC of the Gr flakes.

If it is considered that the Gr flakes are incorporated with interfacial thermal resistance, R_{bd}; then equivalent TC through basal plane [27, 29, 33] with interfacial resistance is given,

$$K_p^{bd} = K_p/(1 + 2R_{bd}K_p/L)$$

…… (10)

where, L is the straight path or equivalent length or contributed length of Gr flake in the suspension (it is expressed as L or L_p^e). So the effective TC enhancement equation 9 can be modified with influence of with interfacial resistance (R_{bd}) can be written expressed as,

$$\frac{K_{eff}}{K_f} = 1 + \frac{2}{3}\varphi \frac{1}{K_f}\left[\frac{K_p}{1 + \frac{2R_{bd}K_p}{L}}\right] \quad \ldots\ldots\ldots\ldots\ldots\ldots (11)$$

Dispersion with carbon based malarial showed the anomalous TC, so homogeneous dispersion can be achieved more easily compared to the solid composites [21, 25].

It is well identified that the graphite is highly anisotropic in thermal conduction. In the basal plane of graphite thermal conductivities is estimated within range from 940 to 2000 W/mK, in contrast TC along the normal to the basal plane is can be varied from only between 5 and 20 W/mK [34]. Even, a larger ratio of basal plane TC to its normal plane can be obtained for the highly oriented pyrolytic graphite [29]. Since few layered Gr flake is the exfoliated peeled off curled graphite structure [8, 35]. For this reason, it is well expected that, Gr flake's TCs through basal plane also would be larger than normal ones. Above observation leads to generate the idea to analysis systematically the experimental data with the effect of anisotropy and not-flatness or non-straightness of Gr flake on the effective TC of the Gr flake dispersion using Maxwell-Garnett effective medium approximation (EMA).

Microscopic observations show that, low loaded uniformly dispersed Gr flakes in base fluid are being far apart from straight or completely flat where basal plane of Gr flake is prevailed as crumpled or non-flat sheets in the dispersion. Because, ultrathin Gr flak able to possess enormously large surface. While its thickness is negligible compare to the straight path in basal plane dimensions of that large surface. A schematic illustration of crumpled or non-flat Gr flake is shown in Figure 2. Gr flakes are highly anisotropy in terms of thermal conduction [6]. It means for Gr flake [in Figure 1b] $K_{11} = K_{22} = K_p >> K_{33}$ so, $K_{11}/K_{33} = K_p/K_{33} >> 1$.

For this reason Gr flakes induce a unique property that individual Gr flake is perfect for thermal conduction path through basal plane with negligible flux loss during the long distance thermal conduction. For non-straight or crumpled Gr flake with non-straight length L_p under a two end temperature difference $\Delta T = T_2 - T_2$ as shown in Figure 2. The thermal flux $q = K_p \Delta T / L_p$ is the thermal transport through basal plane of flat Gr flake.

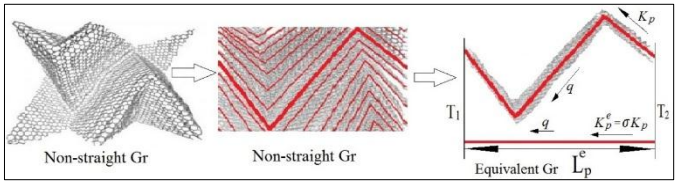

Figure 2: A schematic illustration of the crumpled/ non-flat and equivalent Gr flake.

It can regard that, this Gr flake as equivalent straight thermal flake such that the equal thermal flux q is conducted (Figure 2) between the two ends of the Gr flake in the equivalent straight or flat path distance L_p^e (L). For this reason, the equivalent straight thermal length can relate with flatness/crumpled ratio of usual length $\sigma = L_p^e / L_p$. So the TC of the equivalent straight path is $K_p^e = \sigma K_p$. So the other parameters influenced on the equation 9 also balanced with the flatness/crumpled factor "σ". So, the equation can be modified and expressed as Equation 12.

$$\frac{K_{eff}}{K_f} = 1 + \frac{2}{3}\sigma^2 \varphi \frac{K_p}{K_f} \quad \ldots\ldots\ldots\ldots\ldots\ldots (12)$$

Nomenclature

Gr	Graphene	$\rho(\theta)$	Distribution function describing ellipsoidal particle orientation
NMP	N-Methyl-2-Pyrrolidone	σ	Flatness or crumpled factor
FESEM	Field Emission Scanning Electron Microscopy	**Subscripts**	
DW	Deionized water	K_{ff}	Suspension Effective Thermal Conductivity
TC	Thermal Conductivity	K_p	Thermal Conductivity of the solid particles
EMA	Effective Medium Approach	K_f	Thermal conductivity of base fluids
LPE	Liquid-Phase Exfoliation	X_i	Materials axes

CNT	Carbon Nanotube	a_1, a_2, a_3	Dimensions of the spheroid
EMA	Effective Medium Approximation	L_{ii}	Geometrical factors for the spheroid
MG-EMA	Maxwell Gantt Effective Medium Approximation	R_{bd}	Interfacial thermal resistance
RPM	Revolution per Minute	L_p	Non-straight length of Gr flake
FWHM	Full width at half maximum	ΔT	Two end temperature difference of Gr flake
I	Band intensity of Raman spectrum	q	Thermal flux through basal plane of Gr
IAS	Image Analysis Software	L_p^e or L	Equivalent straight distance of the Gr flake
RMC	Research Management Centre	m_p	Mass contained of the filler
IIUM	International Islamic University Malaysia	μm	Micro meter
		^{o}C	Degree Celsius
Greek symbols			
φ	Volume fraction of filler in base fluid	ml	Mili-litter
∂	Aspect ratio of the ellipsoid	%	Percentage
ρ_p	Density of the dispersed filler material	cm^{-1}	Raman shift
ρ_{bf}	Density of base fluid	W	Watt
β_{ii}	Function of Thermal Conductivity	m	Meter
θ	Angle between materials axis and local particle symmetric axis	K	kelvin

Experimental

Preparation of Gr Dispersed DW Nanofluids

Gr nano-flakes were fabricated using a simple and direct technique sonication assisted liquid phase exfoliation (LPE) of graphite powder in organic solvent N-Methyl-2-Pyrrolidone (NMP). Preparation process is explained elsewhere. For the fabrication of Gr flake, it was carefully maintained the LPE protocol implemented by Khan, et al., (2012) [35]. After fabrication organic solvent was removed from Gr nanosheets using vacuum filtration. Then it was re-dispersed into deionized water (DW). As-produced Gr was suspended as filler into the DW base fluid. Gr suspension in DW is expressed as Gr/DW. After the dispersion of Gr flakes in DW it was bath sonicated using BRANSONIC ultrasonic cleaner for 10 minutes and then stirred about 1hr using magnetic stirrer for the homogenization purpose. Dispersion concentration of the suspension was estimated by UVvis (Thermo Scientific, Multiskan GO) absorbance spectroscopy analysis. Field Emission Scanning Electron Microscopy (FESEM) (Model JEOL JSM-6700F) was used to examine the morphology and size analysis of the as prepared exfoliated Gr flakes. Raman spectroscopy (InVia Reflex, Renishaw, UK) of exfoliated Gr was performed on the prepared films on silicon wafer. Spectra were recorded with 514 nm excitation, within the Raman shift from 1000 to 3200cm^{-1} incorporating with the WiRE 4 software. Image analysis software (IAS) was used for the analysis collected images using OLYMPUS Stream (version 1.9).

Preparation of Gr/DW Nanofluids

For the evaluation TC Gr/DW nanofluid samples were prepared by varying the Gr content DW base fluid. Five different samples were prepared with the volume fraction of 0.10, 0.15, 0.20, 0.25 and 0.30 % of as produced Gr flakes and these volume fractions are mentioned as φ1, φ2, φ3, φ4 and φ5 respectively. Percentage volume fraction of filler in base fluid was calculated using relation in Equation 13.

$$\varphi = \frac{[\frac{m_p}{\rho_p}]}{[\frac{m_p}{\rho_p}]+[\frac{m_{bf}}{\rho_{bf}}]} \times 100\% \quad \text{..... (13)}$$

where, φ is the percentage volume fraction of filler in base fluid. Mass contained of the filler is m_p, density of the dispersed filler material is ρ_p and density of base fluid is ρ_{bf}.

Thermal Conductivity Measurements

Thermal conductivity (TC) of the nanofluids were measured using a KD2 Pro thermal properties analyser (Decagon, USA, version 5), built on the principle of transient hot-wire technique. The KS-1 single-probe sensor was used for these measurements. The accuracy of the instrument is specified by the manufacturer to be within ±5% [36]. Sensor performance was measured with fluid glycerol (recommended and supplied by manufacturer). About 45ml of sample was taken into a close vial. Sensor probe was completely plunged vertically into the sample. Data was taken for every sample at complete equilibrium state. Each data was repeated minimum 10 times (up to 25 times) for the precision purpose. Almost 20% of data were ignored considering them as outliers. Average values were taken for the analysis. After the above-mentioned careful check on the measurement condition and procedure, authors gain strong confidence on the experimental results.

RESULTS AND DISCUSSION

Characterizations

Physical Appearance of Gr/DW Nanofluids

To investigate the effect of volume fraction on TC five different samples of exfoliated Gr dispersion in DW were prepared. Every sample was taken from the supernatant Gr suspensions of final centrifuge speed 500 rpm sample. Figure 3 shows the physical appearance of the exfoliated Gr suspensions in DW. Digital photographs in Figure 3(a-e) show the representative of Gr/DW samples of 500 rpm after preparation of 30 days for the five different volume fractions 0.30, 0.25, 0.20, 0.15 and 0.10 % respectively. A homogeneous and uniform dispersion is acquired. It was apparent that there was no sedimentation in the suspensions.

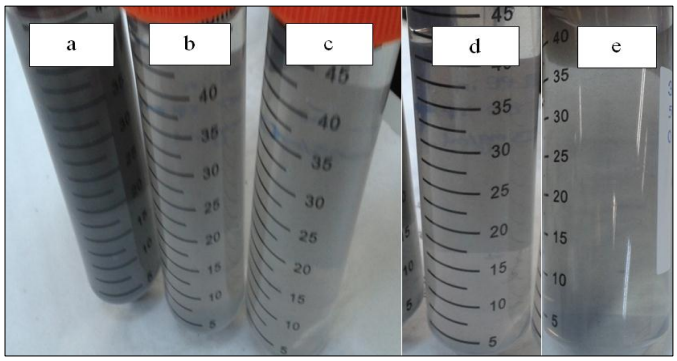

Figure 3: Exfoliated Gr dispersions in DW (Gr/DW). Volume fractions of the samples are: (a) 0.30, (b) 0.25, (c) 0.20, (d) 0.15 and (e) 0.10 %.

FESEM

Figure 4 shows the representative FESEM images of as produced exfoliated Gr sheets. Images were captured on the exfoliated Gr samples of final centrifugation speed 500 rpm. FESEM images in Figure 4a and 4b show the illustrative non-flat or crumpled and folded Gr nanosheets respectively for the exfoliated Gr samples which fell over on one edge with isolated small fragments of Gr on its surface. FESEM analyses of the exfoliated samples revealed the presence of number of flakes stacking. It can be seen that most of the exfoliated flakes are very thin and Gr layers are stacked one over another in an ordered manner [14]. Gr sheets become crumpled due to their negligible thickness with ultra large basal plane surface area surrounded by liquid in suspension.

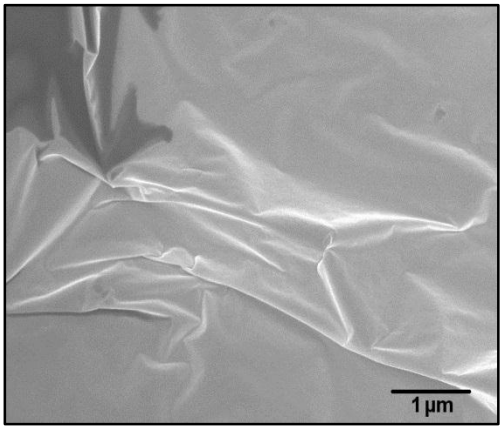

(a)

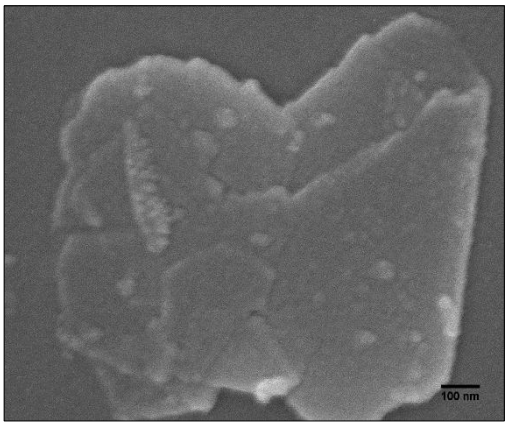

(b)

Figure 4: Representative FESEM images of exfoliated Gr flakes of 500 rpm sample: (a) non-flat or crumpled and (b) folded.

Raman Spectroscopy of Exfoliated Gr

Illustrative of Raman spectrums taken on the LPE precursor graphite powder and sample of exfoliated Gr for final centrifuge speed 500 rpm are shown in Figure 5. The spectrum for the starting precursor powder is presented for the comparison purpose. Three characteristic peaks in the Raman

spectra are appeared. G-band position for exfoliated Gr sample is shifted to slightly higher value than that of the shift (cm^{-1}) of precursor graphite powder. It exposes the change of Gr form the graphite flakes by LPE. Increases in Raman shift (cm^{-1}) of G-band form the precursor graphite is the indication of conversion of graphite to Gr sheets [37]. The sharp G-band in the spectrum of exfoliated Gr sample comprises the Gr sheet; it is for the in-plane vibrational of sp^2 hybridized carbon atoms [37, 38, 39]. Full width at half maximum (FWHM) of 2D-band peak for exfoliated Gr sample is detected around 66 cm^{-1} which endorses the presence of about five-layer Gr in the representative analyzed samples [40]. Relative intensity of D and G band intensity (I_D/I_G) for the precursor graphite powder and the exfoliated Gr are found about 0.599 and 0.697 respectively. It means the starting Graphite powder has the smaller D band intensity than that of exfoliated Gr. It also tells the formation of Gr from the graphite by exfoliation [35, 10].

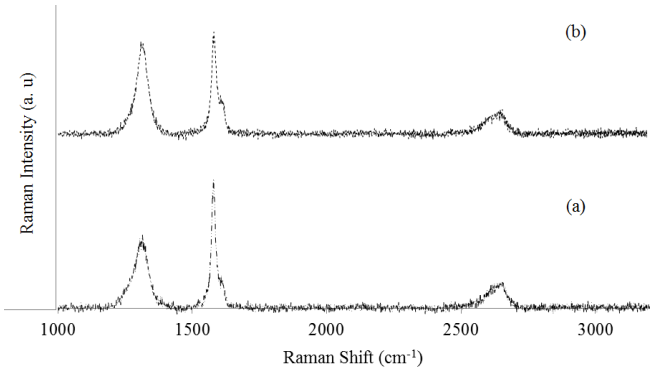

Figure 5: Raman spectra: (a) LPE precursor graphite powder (b) exfoliated Gr of 500 rpm sample.

MODELS PREDICTED AND EXPERIMENTAL TC ENHANCEMENTS OF Gr/DW NANOFLUIDS

Experimental and Maxwell Model Prediction

Relative TC (K_{nf}/K_f) of Gr/DW dispersion samples with the Maxwell predicted TC is presented in Figure 6. Spherical shape of filler is considered in Maxwell effective medium approximation in equation 1. In this model it is considered that the filler Gr is thermally isotropic ($K_{11} = K_{22} = K_{33} = K_p$) with $K_p/K_f >> 1$. In fact, ideal Gr flake is a flat sheet with negligible thickness compare to the flat path dimensions [18]. Moreover, in this analysis it was noted that the values of K_f = 0.604 W/mK and K_p = 3000 W/mK. It is showing that the relative TC values by Maxwell model are about 1 (one) for all samples with increasing volume fraction. It means that predicted TC values for these Gr/DW samples are around similar to the base fluid. It indicated that Maxwell model predicted TC values are terribly underestimates the TC enhancements of Gr/DW nanofluid samples. It directs that there are other mechanisms contribute to the TC enhancement in Gr/DW suspensions. Choi, et al., (2001) [21] also found that the theoretical predictions can show only a minor conductivity enhancement for the carbon base particles suspended nanofluids.

This theoretical model for solid-liquid suspension is originated from the Fourier's law of heat conduction. If it is considered that the thermal diffusion is contributed for the thermal conduction enhancement of carbon based material suspended nanofluids. Then it could presume that the theoretical predictions can increase the TC only very marginally. For this reason, phenomenal experimental results tend to exhibits essential restrictions in orthodox model. These enhancements of TC of Gr suspension in DW can be explained by the two important points. First, type of heat conduction in Gr suspension and other one is type of assembly of Gr sheets and base liquid interface. Current studies discovered that the Gr nanosheets conduct heat by Ballistic flow of phonons [7, 41, 42]. For this reason, Gr nanosheets are likely to dominate the thermal conductivities of the Gr suspended nanofluid. It is considered that in nanofluids ballistic heat conduct in Gr sheets and diffusive heat conduction in DW base fluid [21]. Since ballistic heat conduction is far greater than the thermal diffusion.

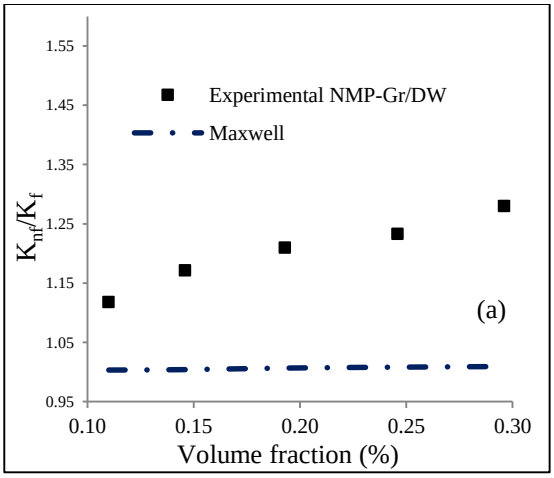

Figure 6: Doted and line graphs for the experimental and Maxwell predicted TC enhancements respectively for the Gr/DW nanofluids.

Experimental with Model-I and Model-II Prediction

With the consideration of flat geometry of Gr flake and their random orientation in base fluid the modified MG-EMA type equation in 9 is mentioned as so called Model-I. It is important to note that the analytical expression in Model-I is precise up to the first order of volume fraction φ as $\varphi \rightarrow 0$. In this expression, it could be included the anisotropy of Gr flake TC through the basal plane and normal to the basal pane $K_{11}/K_f = K_{22}/K_f$ and K_{33}/K_f where all Gr flakes are considered completely flat straight. Actually, only one isotropic TC, K_p is observed for in the Gr flakes. The quite simple relation in equation 9 clearly demonstrates the large TC enhancement induced by the high TC of the Gr flakes. The simple MG-EMA model for the Gr flake is valid for the matrix-based composites in which Gr flakes are surrounded by the matrix. For this type of matrix-based suspension, the

validity of the MG-EMA formula derived above is for very low range of the volume fraction of Gr flakes.

For illustration, Figure 7a shows the comparison between the Model-I (equation 9) and the experimental TC of Gr/DW samples. As seen, the modified simple equation derived mentioned as Model-I by considering flat plate with their random orientation in base fluid from the conventional model which predicts very high TC enhancement than observed in our experimental results. For this reason, the TC enhancement for the dispersion with dilute Gr flakes is not anomalously beyond theoretical predictions. That the TC of the Gr flake suspensions is anomalously greater than the orthodox theoretical predictions (as in Figure 6) is because those models might not be valid for the Gr flake dispersed suspensions.

Higher prediction of TC by Model-I than the experimental results (Figure 7a) suggests that there is still have option for further enhancement in the TC of the Gr based materials by improvement of processing and quality of Gr flake used. The large discrepancies between the predictions and current experiments could be due to interfacial thermal resistance between the base fluid and Gr flakes. Aggregation and non-flatness of the Gr flake in the base fluid could also be reasonably the effect on the TC of the suspension.

The Gr flake and base fluid interfacial thermal contact resistance, R_{bd} can arise from the combination of a poor mechanical or chemical adherence at the interface and other incompatibility and the presence of the Gr flake and base fluid interfacial thermal resistance could result in a drop in the effective TC. To investigate the effect of this R_{bd} on the TC of the suspension the equation 9 is modified as equation 11 and for the explanation purpose it is mentioned as so called Model-II.

In Figure 7b effective TC of Model-II and experimental results of Gr/DW nanofluids samples are plotted. In this figure, it is also seen that the predicted thermal conductivities are also highly over predicted than the experimental values. For the calculation effective TC using Model-II the value of R_{bd} is considered 2.89×10^{-9} m^2KW^{-1} by considering all the Gr flakes are completely flat. Although estimated value of interfacial thermal resistance between Gr and solid epoxy matrix is 3.5×10^{-9} m^2KW^{-1} [18]. As our matrix is base fluid DW, for this reason it is seen by tuning that, for the interfacial resistance, $R_{bd} = 2.89 \times 10^{-9}$ m^2KW^{-1} the closest value of effective TC was obtained with the experimental data. So, it reveals that there is a negligible interfacial resistance prevailed between the Gr flake and base fluid. So it could be said that, almost there is no effect of interfacial resistance is observed on the effective TC of the Gr/DW nanofluids samples.

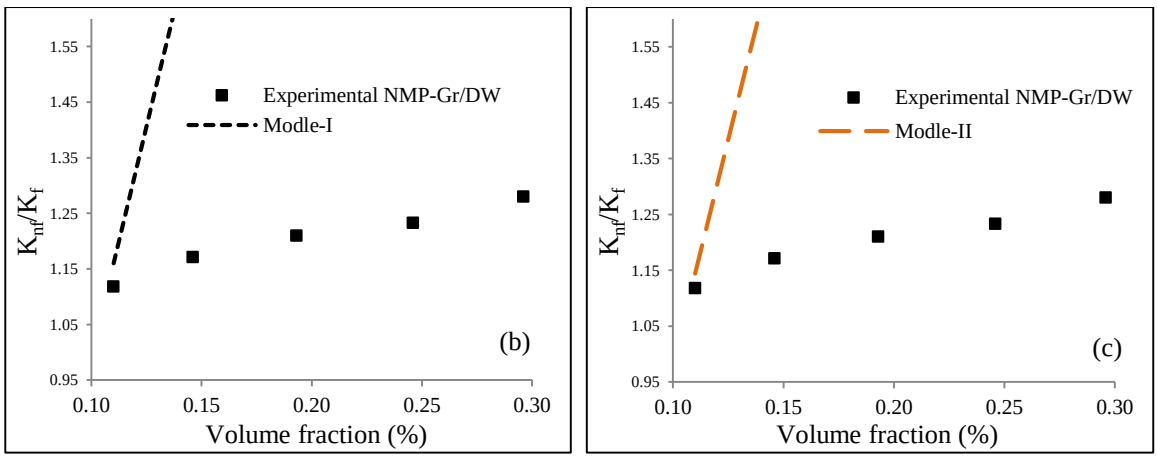

Figure 7: Doted and line graphs for the experimental and predicted TC enhancements respectively for the Gr/DW nanofluids: (a) Experimental with Model-I, (b) Experimental with Model-II.

Experimental with Model-III with Crumple-ness of Gr Flakes

Microscopic observations show that, low loaded uniformly dispersed Gr flakes in base fluid are being far apart from straight or completely flat where basal plane of Gr flake is prevailed as crumpled or non-flat sheets in the dispersion. Because, ultrathin Gr flak able to possess enormously large surface. Its thickness is negligible compare to the straight path in basal plane dimensions of that large surface.

From the above observation, expression in Equation 9 is modified by implementing the flatness or crumpled factor (σ) for Gr flake dispersed nanofluid as in Equation 12 (as explained above). In the explanation Equation 12 is mentioned as so called Model-III. Effective TC enhancements form Model-III and the experimental results of Gr/DW nanofluids samples are plotted in Figure 8. The results shown in Figure 8 indicate that the prediction with non-flatness or crumpled factor, σ = ~ 0.185 in modified Model-III gives the effective thermal conductivities that agree well with the measured TC enhancements. Tuning the value of non-flatness or crumpled factor, it is seen that larger the values of σ lead to better thermal enhancement effects shown in Figure 9.

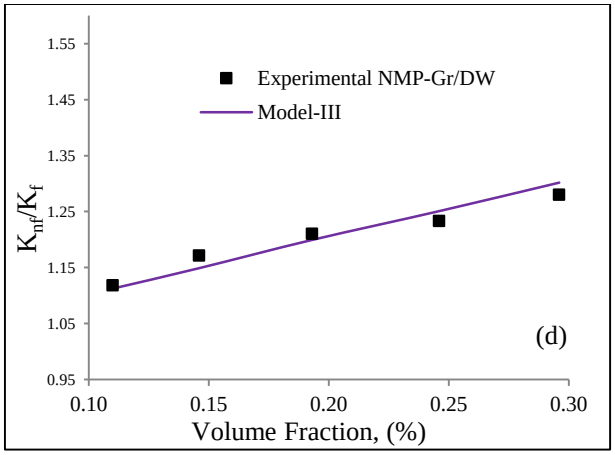

Figure 8: Doted and line graphs for the experimental and Model-III predicted TC enhancements respectively for the Gr/DW nanofluids.

At the analysis of filler Gr flake dispersion in DW, it is also seen that at the similar value of σ predicted TC enhancements of Model-III is reasonably agreed with the measured TC enhancement for the same Gr flakes. Experimentally it was estimated the crumpled factor by analyzing the non-straightness or non-flatness of exfoliated Gr flakes. It was conducted the measurements of about 50 non-flat including crumpled or folded Gr flakes using image analysis software (IAS). Ratio of equivalent or lateral lengths and non-straight lengths ($\sigma = L_p^e / L_p$) (mentioned as crumpled or non-straightness factor), was estimated by individually dividing the measured value of L_p^e by the value of L_p for the flakes. From the analysis average value of this ratio was perceived about 0.244.

Instead, non-flatness or crumpled factor is originated from the non-flatness of Gr flake integrated in Model-III. This factor could vary from zero to one (1). If the non-flatness or crumpled factor is zero than the equivalent or contributed length also will be zero and if it is one then the equivalent or contributed length will be same as straight path length of Gr flake. Figure 9 shows the effect of non-flatness or crumpled factor on the TC enhancements of Gr/DW suspension for every volume fraction using Model-III. Tuning the values of non-flatness or crumpled factor, it is seen that larger the values of σ (closer to one) lead to better thermal enhancement effects and when σ equal one, it gives the TC enhancements by Model-I which is highly over predicted than the experimental TC enhancements (as shown in Figure 7a).

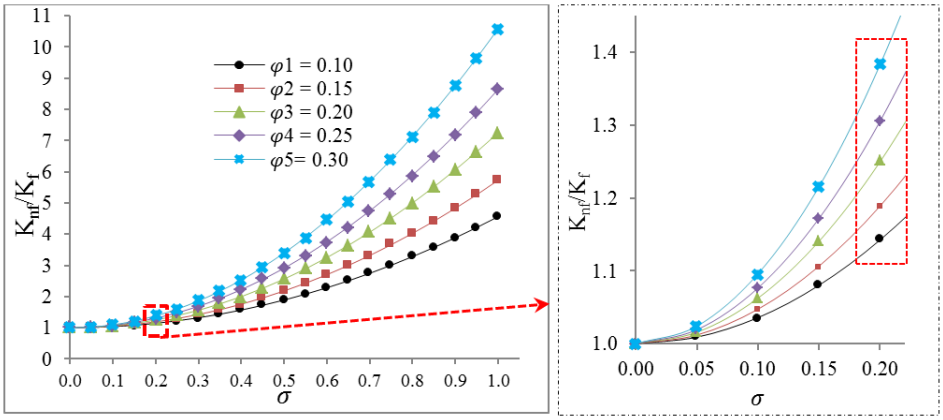

Figure 9: The effect of non-flatness or crumpled factor (σ) on the TC enhancements of Gr/DW suspension for using Model-III.

CONCLUSIONS

In this study, the analytical effective medium theories were successfully modified for predicting the TC enhancements of Gr flake dispersed nanofluids with the consideration of low filling of Gr flake in the base fluids. Experimentally it is perceived that, higher volume fraction of filler provided the higher TC enhancements of water based exfoliated Gr flake dispersed nanofluids (Gr/DW). Well agreement was perceived between the experimentally attained data and the predicted values by implementing modified model. It revealed that Gr's negligible thickness compared to its extremely wide basal plane dimensions and non-flatness or crumpled geometry of the Gr flakes in base fluid have the leading impacts to the effective TC properties of Gr flake dispersed nanofluids.

ACKNOWLEDGEMENT

Authors are grateful to the Research Management Centre (RMC), International Islamic University Malaysia (IIUM) for all kinds of support to accomplish this research work.

REFERENCES

[1] Zenghu, H. (2008). *Nanofluids with Enhanced Thermal Transport Properties* (Doctoral dissertation, Ph. D. thesis, University of Maryland).

[2] Xie, H., Yu, W., Li, Y., & Chen, L. (2011). Discussion on the thermal conductivity enhancement of nanofluids. *Nanoscale research letters*, *6*(1), 1.

[3] Maxwell, J. C. (1881). *A treatise on electricity and magnetism* (Vol. 1). Clarendon press.

[4] Novoselov, K. S., Geim, A. K., Morozov, S. V., Jiang, D., Zhang, Y., Dubonos, S. V., ... & Firsov, A. A. (2004). Electric field effect in atomically thin carbon films. *science*, *306*(5696), 666-669.

[5] Sanchez, V. C., Jachak, A., Hurt, R. H., & Kane, A. B. (2011). Biological interactions of graphene-family nanomaterials: an interdisciplinary review. *Chemical research in toxicology*, *25*(1), 15-34.

[6] Yu, W., Xie, H., & Chen, W. (2010). Experimental investigation on thermal conductivity of nanofluids containing graphene oxide nanosheets. *Journal of Applied Physics*, *107*(9), 094317.

[7] Munoz, E., Lu, J., & Yakobson, B. I. (2010). Ballistic thermal conductance of graphene ribbons. Nano letters, 10(5), 1652-1656.

[8] Hernandez, Y., Nicolosi, V., Lotya, M., Blighe, F. M., Sun, Z., De, S., Krishnamurthy, S., Goodhue, R., Hutchison, J., Scardaci, V., Ferrari, A. C. & Coleman, J. N. (2008). High-yield production of graphene by liquid-phase exfoliation of graphite. *Nature Nanotechnology*, *3*(9), 563-568.

[9] Paredes, J. I., Villar-Rodil, S., Solís-Fernández, P., Fernández-Merino, M. J., Guardia, L., Martínez-Alonso, A., & Tascón, J. M. D. (2012). Preparation, characterization and fundamental studies on graphenes by liquid-phase processing of graphite. *Journal of Alloys and Compounds*, *536*, S450-S455.

[10] Lotya, M., Hernandez, Y., King, P. J., Smith, R. J., Nicolosi, V., Karlsson, L. S., ... & Duesberg, G. S. (2010). Liquid phase production of graphene by exfoliation of graphite in surfactant/water solutions. *Journal of the American Chemical Society*, *131*(10), 3611-3620.

[11] Coleman, J. N. (2012). Liquid exfoliation of defect-free graphene. *Accounts of chemical research*, *46*(1), 14-22.

[12] Ciesielski, A., & Samorì, P. (2014). Graphene via sonication assisted liquid-phase exfoliation. *Chemical Society Reviews*, *43*(1), 381-398.

[13] Arao, Y., Mizuno, Y., Araki, K., & Kubouchi, M. (2016). Mass production of high-aspect-ratio few-layer-graphene by high-speed laminar flow. *Carbon*, *102*, 330-338.

[14] Vadukumpully, S., Paul, J., & Valiyaveettil, S. (2009). Cationic surfactant mediated exfoliation of graphite into graphene flakes. *Carbon*, *47*(14), 3288-3294.

[15] Balandin, A. A., Ghosh, S., Bao, W., Calizo, I., Teweldebrhan, D., Miao, F., & Lau, C. N. (2008). Superior thermal conductivity of single-layer graphene. *Nano letters*, *8*(3), 902-907.

[16] Balandin, A. A. (2011). Thermal properties of graphene and nanostructured carbon materials. *Nature materials*, *10*(8), 569-581.

[17] Kim, P., Shi, L., Majumdar, A., & McEuen, P. L. (2001). Thermal transport measurements of individual multiwalled nanotubes. *Physical review letters*, *87*(21), 215502.

[18] Shahil, K. M., & Balandin, A. A. (2012). Graphene-multilayer graphene nanocomposites as highly efficient thermal interface materials. *Nano letters*, *12*(2), 861-867.

[19] Huxtable, S. T., Cahill, D. G., Shenogin, S., Xue, L., Ozisik, R., Barone, P., ... & Keblinski, P. (2003). Interfacial heat flow in carbon nanotube suspensions. *Nature materials*, *2*(11), 731-734.

[20] Baby, T. T., & Ramaprabhu, S. (2010). Investigation of thermal and electrical conductivity of graphene based nanofluids. *Journal of Applied Physics*, *108*(12), 124308.

[21] Choi, S. U. S., Zhang, Z. G., Yu, W., Lockwood, F. E., & Grulke, E. A. (2001). Anomalous thermal conductivity enhancement in nanotube suspensions. *Applied physics letters*, *79*(14), 2252-2254.

[22] Chen, T., Weng, G. J., & Liu, W. C. (2005). Effect of Kapitza contact and consideration of tube-end transport on the effective conductivity in nanotube-based composites. *Journal of applied physics*, *97*(10), 104312.

[23] Murshed, S. S., de Castro, C. N., Sohel Murshed, S. M., & de Castro, C. A. N. (2011, July). Contribution of Brownian motion in thermal conductivity of nanofluids. In *Proc World Congress on Engineering* (pp. 1905-1909).

[24] Nan, C. W. (1993). Physics of inhomogeneous inorganic materials. *Progress in Materials Science*, *37*(1), 1-116.

[25] Nan, C. W., Shi, Z., & Lin, Y. (2003). A simple model for thermal conductivity of carbon nanotube-based composites. *Chemical Physics Letters*, *375*(5), 666-669.

[26] Nan, C. W., Birringer, R., Clarke, D. R., & Gleiter, H. (1997). Effective thermal conductivity of particulate composites with interfacial thermal resistance. *Journal of Applied Physics*, *81*(10), 6692-6699.

[27] Nan, C. W., Liu, G., Lin, Y., & Li, M. (2004). Interface effect on thermal conductivity of carbon nanotube composites. *Applied Physics Letters*, *85*(16), 3549-3551.

[28] Nan, C. W. (1994). Effective-medium theory of piezoelectric composites. *Journal of applied physics*, *76*(2), 1155-1163.

[29] Deng, F., Zheng, Q. S., Wang, L. F., & Nan, C. W. (2007). Effects of anisotropy, aspect ratio, and nonstraightness of carbon nanotubes on thermal conductivity of carbon nanotube composites. *Applied Physics Letters*, *90*(2), 021914.

[30] Nan, C. W., Li, X. P., & Birringer, R. (2000). Inverse problem for composites with imperfect interface: determination of interfacial thermal resistance, thermal conductivity of constituents, and microstructural parameters. *Journal of the American Ceramic Society*, *83*(4), 848-854.

[31] Wang, S., Zhang, Y., Abidi, N., & Cabrales, L. (2009). Wettability and surface free energy of graphene films. *Langmuir*, *25*(18), 11078-11081.

[32] Benveniste, Y., & Miloh, T. (1986). The effective conductivity of composites with imperfect thermal contact at constituent interfaces. *International Journal of Engineering Science*, *24*(9), 1537-1552.

[33] Bryning, M. B., Milkie, D. E., Islam, M. F., Kikkawa, J. M., & Yodh, A. G. (2005). Thermal conductivity and interfacial resistance in single-wall carbon nanotube epoxy composites. *Applied Physics Letters*, *87*(16), 161909.

[34] Cahn, R. W. (1983). Physics of graphite: BT Kelly (Applied Science Publishers, London, 1981) pp. 477. price:£ 48.

[35] Khan, U., O'Neill, A., Porwal, H., May, P., Nawaz, K., & Coleman, J. N. (2012). Size selection of dispersed, exfoliated graphene flakes by controlled centrifugation. *Carbon*, *50*(2), 470-475.

[36] Decagon, D. (2006). KD2 Pro Theory. *KD2 Pro User Manual*.

[37] Hodkiewicz, J. (2010). Characterizing graphene with Raman spectroscopy. *Thermo Scientific application note*, *51946*.

[38] Wojtoniszak, M., Chen, X., Kalenczuk, R. J., Wajda, A., Łapczuk, J., Kurzewski, M., ... & Borowiak-Palen, E. (2012). Synthesis, dispersion, and cytocompatibility of graphene oxide and reduced graphene oxide. *Colloids and Surfaces B: Biointerfaces*, *89*, 79-85.

[39] Ferrari, A. C., & Basko, D. M. (2013). Raman spectroscopy as a versatile tool for studying the properties of graphene. *Nature nanotechnology*, *8*(4), 235-246.

[40] Hao, Y., Wang, Y., Wang, L., Ni, Z., Wang, Z., Wang, R., ... & Thong, J. T. (2010). Probing Layer Number and Stacking Order of Few-Layer Graphene by Raman Spectroscopy. *small*, *6*(2), 195-200.

[41] Hone, J., Whitney, M., Piskoti, C., & Zettl, A. (1999). Thermal conductivity of single-walled carbon nanotubes. *Physical Review B*, *59*(4), R2514.

[42] Savin, A. V., Kivshar, Y. S., & Hu, B. (2010). Suppression of thermal conductivity in graphene nanoribbons with rough edges. *Physical Review B*, *82*(19), 195422.